z-scan measurement of the nonlinear absorption of a thin gold film

David D. Smith[a)]
NASA Marshall Space Flight Center, Space Sciences Laboratory, SD48, Huntsville, Alabama 35812

Youngkwon Yoon and Robert W. Boyd
University of Rochester, Institute of Optics, Rochester, New York 14627

Joseph K. Campbell, Lane A. Baker, and Richard M. Crooks
Texas A&M University, Department of Chemistry, College Station, P.O. Box 30012, Texas 77842-3012

Michael George
University of Alabama in Huntsville, Department of Chemistry, Huntsville, Alabama 35899

(Received 5 April 1999; accepted for publication 1 September 1999)

We have used the *z*-scan technique at a wavelength (532 nm) near the transmission window of bulk gold to measure the nonlinear absorption coefficient of continuous approximately 50-Å-thick gold films, deposited onto surface-modified quartz substrates. For highly absorbing media such as metals, we demonstrate that determination of either the real or imaginary part of the third-order susceptibility requires a measurement of both nonlinear absorption and nonlinear refraction, i.e., both open- and closed-aperture *z* scans must be performed. Closed-aperture *z* scans did not yield a sufficient signal for the determination of the nonlinear refraction. However, open-aperture *z* scans yielded values ranging from $\beta = 1.9 \times 10^{-3}$ to 5.3×10^{-3} cm/W in good agreement with predictions which ascribe the nonlinear response to a Fermi smearing mechanism. We note that the sign of the nonlinearity is reversed from that of gold nanoparticle composites, in accordance with the predictions of mean field theories. © *1999 American Institute of Physics.* [S0021-8979(99)06523-8]

INTRODUCTION

Gold nanoparticle composite materials are known to display large optical nonlinearities.[1–6] In order to assess the validity of generalized effective medium theories (particularly the Maxwell Garnett model) for describing the linear and nonlinear optical properties of metal nanoparticle composites, knowledge of the linear and nonlinear susceptibilities of the constituent materials is a prerequisite. For the dielectric constituent the measurement of these properties is relatively straightforward. However, measurement of the ''inherent'' nonlinear susceptibility of the metal is more difficult. In previous studies the nonlinearity of the metal itself was deduced from measurements on the composite as a whole, by comparing the nonlinear susceptibility of the composite to the predictions of the effective medium theory believed to be accurate for the particular system considered.[3–6] Typically for gold a value of $\mathrm{Im}\,\chi_i^{(3)} \approx 10^{-7}$ esu was obtained, which corresponds very closely to the theoretical value for the Fermi smearing mechanism derived by Hache *et al.*[6] However, the fact that the value of $\mathrm{Im}\,\chi_i^{(3)}$ is deduced from the very theory in question, rather than measured directly, casts a certain doubt over the applicability of the theory simply due to the circular nature of the deduction.

In this study the inherent nonlinearity of the metal is measured directly using very thin gold films. Standard vapor deposited gold films must be as thick as several hundred angstroms to be continuous and uniform.[7] However, at these thicknesses these films have transmittance values that are too low to obtain a significant signal from a *z* scan. Moreover, the films are easily damaged. To overcome these problems we used a quartz substrate modified with a self-assembled monolayer (SAM) that promotes the formation of a more uniform and more robust gold coating. SAMs have the advantage over the relatively thick transition metal undercoatings (usually Cr, Ti, or W) that are typically applied to promote adhesion, in that they do not change the optical properties of the sample,[8] which is of particular importance when the sample thickness is comparable to that of the prelayer. For example, a 50 Å layer of Au requires a 50 Å prelayer of Cr which can significantly alter the linear and nonlinear optical properties of the sample. Additionally, to further increase the signal to noise ratio, we performed the measurements at a wavelength very near the transmission window of bulk gold (~500 nm). This transmission window occurs between the threshold for interband absorption and the onset of long-wavelength reflection. For films that are thick enough to be continuous there is no ''anomalous absorption'' feature or ''dielectric anomaly'' (there is no surface plasmon resonance), as is evident in films that are thin enough to consist mainly of granular islands.[9]

EXPERIMENTAL PROCEDURE

A 50 Å layer of Au on quartz was prepared following the procedure of Goss *et al.*[8,10,11] The procedure essentially consists of forming an adhesion layer of (3-mercaptopropyl) trimethoxysilane MPS on a quartz substrate which has been

a)Electronic mail: david.d.smith@msfc.nasa.gov

cleaned with H_2O_2/H_2SO_4 (piranha) solution, followed by vacuum evaporation or sputtering of Au onto this surface. The thiol groups of the MPS bind strongly to the Au coating, resulting in a more uniform and durable coating. Atomic force microscopy (AFM), scanning tunneling microscopy (STM), conductivity, and transmittance measurements were performed on a 50-Å-thick vapor-deposited sample to examine the continuity of the film. The nonlinearity was determined by *z*-scan measurements on a 50-Å-thick vapor-deposited film and an 85-Å-thick sputter-deposited film.

z scan[12] is a simple, sensitive technique which relies on the transformation of nonlinear phase shifts into far-field amplitude deflections to obtain the complex nonlinear refractive index $n_2 = n_2' + in_2''$. It is essentially a derivative of the ubiquitous single-beam-power-in versus power-out transmission measurement[13] but attains greater efficiency by focusing the beam and translating the sample. The technique involves the measurement of the transmittance through an aperture placed in the far field as the sample is translated through the focus of a Gaussian beam. For a sufficiently small aperture, this procedure provides a measurement of the real part of the nonlinear refractive index n_2'. If the aperture is fully opened so that the detector collects all the light, then the *z* scan provides a measurement of the imaginary part of the nonlinear refractive index n_2'' or, alternatively, the nonlinear absorption coefficient β. If $\beta > 0$, then the *z* scan will result in a trough, indicative of induced absorption. If $\beta < 0$, then the *z* scan will produce a peak, indicating induced transparency. Since all the flux from the sample is collected at the detector, the transmitted power may be calculated without having to perform the free-space Fresnel propagation to the aperture. The normalized transmittance may be expressed as[12]

$$T(z) = \sum_{m=0}^{\infty} \frac{\left[\dfrac{-\beta I_0 L_{\text{eff}}}{1 + z^2/z_0^2}\right]^m}{(m+1)^{3/2}}, \tag{1}$$

where *z* is the longitudinal displacement of the sample from the focus, β is the nonlinear absorption coefficient, I_0 is the on-axis peak intensity at the focus, L_{eff} is the effective interaction length, z_0 is the Rayleigh diffraction length, and the temporal profile of the pulse has been assumed to be Gaussian. Typically, if the series converges, only the first few terms are needed for numerical evaluation. Hence, the coefficient β may be determined from a fit of this expression to the empirical data.

We performed open- and closed-aperture *z* scans at various peak intensities to characterize the nonlinear absorption and refraction for both a 50-Å-thick vapor-deposited Au film and an 85-Å-thick sputter-deposited film. Low intensity scans provided a control that could be used to subtract out any linear effects which might modify the *z*-scan profile. A frequency doubled Nd: yttrium–aluminum–garnet laser at 532 nm provided 30 ps mode-locked pulses at a repetition rate of 10 Hz. The Au films were placed on a track near the focus of the beam. The focal length of the lens was 100 cm and the full width at half maximum beam diameter incident on the lens was 2.5 mm. The beam waist and Rayleigh diffraction length were measured independently with a knife edge and found to be $w_0 = 63\ \mu$m and $z_0 = 30.5$ mm, respectively. The refractive index and nondimensional extinction coefficient of the film were found from an interpolation of the data of Theye[14,15] for bulk Au, and were taken as $n = 0.45$ and $k = 2.42$, respectively. Hence, the absorption coefficient and effective interaction length were $\alpha = 5.72 \times 10^5\ \text{cm}^{-1}$ and $L_{\text{eff}} = 4.35$ nm, respectively.

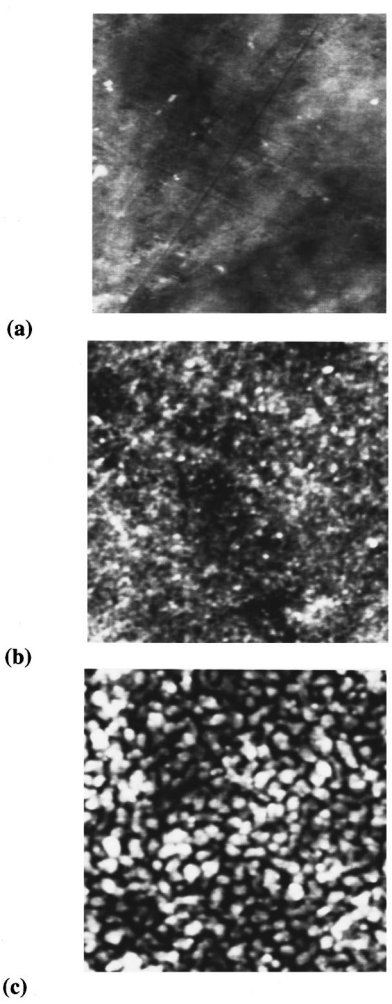

FIG. 1. AFM images of (a) the untreated polished quartz substrate, (b) the MPS treated substrate, and (c) the gold-coated MPS surface. The scan size is $1 \times 1\ \mu$m.

RESULTS AND DISCUSSION

AFM images obtained in tapping mode reveal that the morphology of the gold film is characteristic of continuous metal films. Figure 1 shows $1 \times 1\ \mu$m AFM scans of the sample at three different stages in the preparation process. AFM images of the polished quartz substrate prior to MPS coating [Fig. 1(a)], the MPS coated substrate surface without the gold layer [Fig. 1(b)], and the vapor-deposited gold film [Fig. 1(c)] are shown. The morphology of the quartz substrate is typical for polished glass samples. Scratches from the polishing process are visible. However, these substrates were very flat with a rms roughness of 4.3 Å. In order to compare the gold-coated with the MPS-coated regions of the quartz, images were obtained from the same sample. The

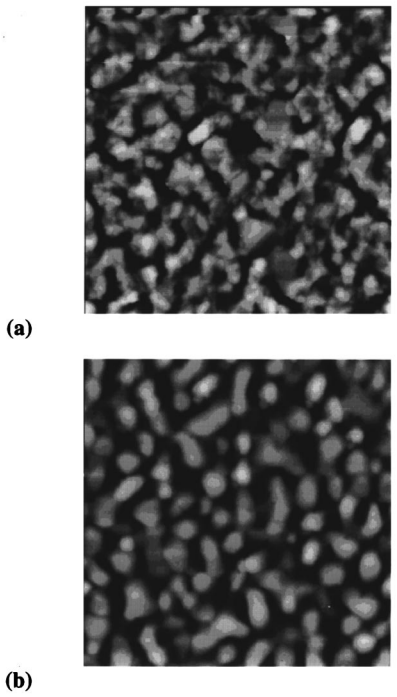

FIG. 2. STM images of (a) 75 Å Au film on MPS modified quartz and (b) a reference 2000 Å Au layer on 100 Å of Ti on a silicon substrate. The scan size is $0.5\times0.5\ \mu$m.

MPS region without the gold film had a rms roughness of 4.5 Å with a mean particle diameter of 15 nm. The gold-coated region had a morphology typical of continuous metal films with a rms roughness of 16.6 Å and an average grain diameter of 50 nm. The granular surface observed for the MPS-coated sample may provide abundant nucleation sites for gold film growth. This would promote the growth of the very thin continuous polycrystalline gold film that we observe for this process. Deposition of gold onto an untreated quartz substrate, on the other hand, would have resulted in a discontinuous film common for very thin ($<$15 nm) gold films where gold–gold cohesive interactions predominate leading to island-like structures.

The conductivity of the 50 Å Au film was measured by the four point method,[16] and determined to be bulk-like. The resistivity varied for different spots on the sample between about 0.5 and 100 times the bulk value. It was difficult to get reproducible values for the resistivity, however, because the probe tips easily penetrated the thin Au layer.

STM images obtained with a platinum/iridium tip at a scan size of $0.5\times0.5\ \mu$m are shown in Fig. 2 for the thin Au/MPS/quartz sample and for a thick Au reference. A 2000 Å layer of Au on a silicon substrate with a 100 Å pre-layer of Ti was used as the reference. Note that the morphologies are essentially identical except for the appearance of considerable substructure in the thinner sample [Fig. 2(a)]. The additional substructure appears because the film thickness is much smaller than the width of the surface features. The rms surface roughness is similar for the two cases (35 Å for the Au/MPS/quartz sample, and 25 Å for the Au/Ti/silicon reference) with crystallite sizes of approximately 50 nm (note that the film thickness is only 5 nm). The fact that the STM probe tip did not crash into the surface during scanning due to a dramatic decrease in tunneling current is an indication that the film is continuous. A tip crash would occur if the tip is scanned from an area covered by gold onto an area where the insulating quartz substrate may show through. Hence, although boundaries are observed, from an electrical (i.e., optical) standpoint the film is continuous because the boundaries do not drastically reduce the current resulting in a tip crash. In addition, x-ray photoelectron spectroscopy did not reveal a silicon peak, consistent with the STM results.

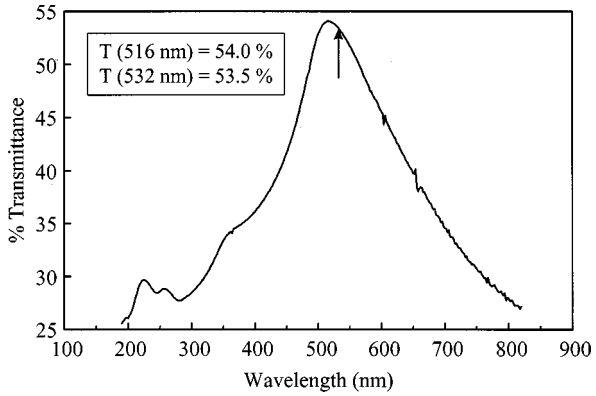

FIG. 3. Transmittance spectrum of 50 Å Au film. The arrow corresponds to the wavelength at which the z scan was performed.

The transmittance spectrum of the 50 Å Au film was measured between 190 and 820 nm using a UV-visible diode array spectrophotometer and is shown in Fig. 3. Note that rather than displaying the dipolar plasmon resonance usually associated with a metal colloid or composite, there is a transmission window with a peak at 516 nm, which is characteristic of Au films that are continuous and is in agreement with the theoretical predictions of Sheng[17] for Au composites above the percolation threshold. At the wavelength of the experiment, 532 nm, the transmission is 53.5% which is close to the maximum of 54% at 516 nm and permits a sufficient signal to noise ratio for a z scan to be performed.

Because the nonlinearity of metal nanoparticles is thought to arise primarily from absorptive mechanisms[6] open-aperture z scans were performed initially. A typical open-aperture z scan on the vapor-deposited Au film is shown in Fig. 4. The error bars represent the standard devia-

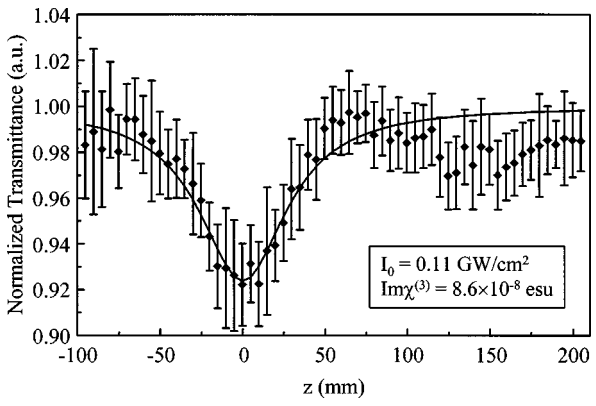

FIG. 4. Open-aperture z scan of 50 Å Au film.

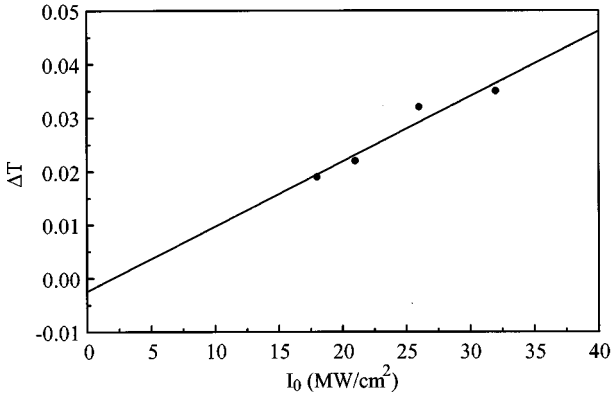

FIG. 5. Change in transmittance ΔT vs peak on-axis intensity at the focus for a sputtered Au film. For a pure third-order effect the data should fall on a straight line and extrapolate to $\Delta T=0$ at zero intensity.

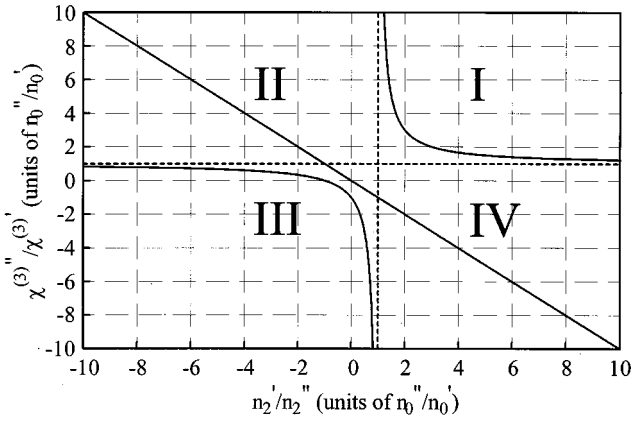

FIG. 6. Coupling of the complex cubic susceptibility to the complex nonlinear refractive index. The line indicates the solution in the limit of large absorption ($n_0'' \gg n_0'$). In general the solution is a hyperbola which for lossless media ($n_0'' \ll n_0'$) is centered about the origin, whereas for significantly absorbing media it is shifted with respect to the origin as shown here. When the solution extends into the fourth or second quadrants a sign reversal occurs in the imaginary or real component, respectively, upon transformation from phenomenological to theoretical quantities.

tion of 20 shots. The incident peak power was $P_i=8.6\,\mathrm{kW}$ corresponding to $I_0=110\,\mathrm{MW/cm^2}$. For intensities greater than 160 $\mathrm{MW/cm^2}$ ablative damage typically occurred which was evident by a sharp peak in the *z*-scan transmission which increased with each scan, as well as an asymmetry in the baseline. Equation (1) was used to fit a curve to the data by varying the adjustable parameter β. For this spot the best fit yields a value of $\beta=5.3\times10^{-3}\,\mathrm{cm/W}$. Note that as the focus is approached, the transmittance decreases indicating that the metal is an induced absorber, the opposite effect from that obtained for metal colloids or composites (below the percolation threshold). For the vapor-deposited film the nonlinear absorption coefficient varied from $\beta=1.9\times10^{-3}$ to $5.3\times10^{-3}\,\mathrm{cm/W}$ depending on the spot. If we naively neglect nonlinear refraction and transform these values to susceptibilities we obtain a range of $\mathrm{Im}\,\chi_i^{(3)}=3.2\times10^{-8}$ to $8.6\times10^{-8}\,\mathrm{esu}$. However, we will soon show that for metals $\mathrm{Im}\,\chi_i^{(3)}$ cannot be calculated so simply.

By its nature *z* scan is a power-dependent study and higher-order effects are often evident by their effect on the *z*-scan profile (for the *z* scan of Fig. 4 higher-order effects are just becoming evident); however, they are made even more evident by varying I_0. The result of a power-dependent study on the 85 Å sputter-deposited Au film is shown in Fig. 5. The data falls on a straight line and extrapolates to a change in the normalized transmittance of $\Delta T=0$ at zero intensity indicating a pure third-order effect. At this particular spot on the sample the nonlinear absorption coefficient varied from $\beta=3.7\times10^{-3}$ to $4.5\times10^{-3}\,\mathrm{cm/W}$ as the intensity was varied, much less than the spot-to-spot variation. Below approximately $I_0=100\,\mathrm{MW/cm^2}$ no higher-order effects were evident in these films.

Closed-aperture *z* scans were also performed to obtain n_2. However, a signal exceeding the noise level (S/N>1) could not be resolved. In place of a direct empirical determination of n_2' for the gold film we can still gain insight into the value of the refractive nonlinearity however, through deduction from measurements on composites and because the strong absorption in a metal provides a coupling between real and imaginary quantities (between $\mathrm{Im}\,\chi^{(3)}$ and n_2' and between $\mathrm{Re}\,\chi^{(3)}$ and n_2'') when transforming from experimental quantities to susceptibilities.

In general susceptibilities may not be measured directly but must be deduced through experimental determination of the refractive index *n*, where *n* is both complex and nonlinear. Determination of the real or imaginary part of the linear susceptibility requires a measurement of both n_0' and n_0''. Similarly, specification of the full complex nonlinear susceptibility requires a measurement of both n_2' and n_2'', where in general there is a coupling between the real (imaginary) part of n_2 and the imaginary (real) part of $\chi^{(3)}$ that arises from the complex nature of the linear refractive index n_0. This coupling is usually not considered in nonlinear optics measurements, however, it becomes particularly significant for highly absorptive materials (i.e., metals). The proper equation (in electrostatic units) relating the phenomenological and theoretical quantities is

$$n_2=\frac{12\pi^2\chi^{(3)}}{n_0 n_0' c}. \tag{2}$$

Equation (2) contains two powers of the linear refractive index n_0, one of which comes from the driven nonlinear wave equation and is complex, the other which comes from the Poynting vector and is by necessity real. Hence, the real and imaginary parts of the cubic susceptibility are

$$\chi^{(3)'}=\frac{n_0' c}{12\pi^2}(n_0' n_2'-n_0'' n_2''), \tag{3}$$

$$\chi^{(3)''}=\frac{n_0' c}{12\pi^2}(n_0' n_2''+n_0'' n_2'). \tag{4}$$

Dividing Eq. (4) by Eq. (3) we obtain the equation of a hyperbola with asymptotes displaced along the ordinate and abscissa by n_0''/n_0' and intersecting the axes at $-n_0'/n_0''$ as shown in Fig. 6. The second term on the right-hand side of these equations determines whether a sign reversal occurs

upon transformation from refractive indices to susceptibilities. The general condition for a sign reversal to occur in the imaginary component is

$$|n_0' n_2''| < |n_0'' n_2'| \quad \text{and} \quad \frac{n_2'}{n_2''} < 0 \tag{5}$$

and similarly for the real component the condition is

$$|n_0' n_2'| < |n_0'' n_2''| \quad \text{and} \quad \frac{n_2'}{n_2''} > 0. \tag{6}$$

Obviously both of these conditions cannot be met simultaneously since they are true in different half planes. The first condition, however, specifies the second quadrant, while the second condition specifies the fourth quadrant. No sign reversal occurs in the first or third quadrants. Hence, the sign reversal occurs in the imaginary component in the second quadrant, and in the real component in the fourth quadrant. Note that when $n_0'' \gg n_0'$ (absorption dominates) the solution collapses to a straight line such that

$$\frac{\chi^{(3)''}}{\chi^{(3)'}} = -\frac{n_2'}{n_2''}. \tag{7}$$

In this case there will always be a sign reversal in one of the components when transforming between the theoretical and phenomenological quantities since the solution always lies either in the second or fourth quadrants. In the opposite limit, however, when $n_0'' \ll n_0'$, absorption may be neglected and the solution reduces to a hyperbola centered about the origin

$$\frac{\chi^{(3)''}}{\chi^{(3)'}} \frac{n_2'}{n_2''} = 1. \tag{8}$$

In this case the solution remains within the first and third quadrants so that there is no sign reversal in the components and the coupling (provided by n_0) may be neglected. Between these limits is the case of a good conductor $n_0'' \approx n_0'$ and we obtain the hyperbola shown in Fig. 6. In this case the part of the hyperbola that extends into the second and fourth quadrants defines the conditions that lead to a sign reversal in either the imaginary or the real component (but not both), respectively.

For the specific case of gold at 532 nm the real and imaginary parts of the linear refractive index are related by $n_0'' \approx 5 n_0'$ so that a significant part of the hyperbola extends into the quadrants which lead to a sign reversal. *z*-scan measurements performed on a gold doped composite glass [$n_0'' \ll n_0'$, no coupling as in Eq. (8)] indicated that the effective nonlinear susceptibility of the composite is $\chi^{(3)} = (8 \times 10^{-12} - 4 \times 10^{-11} i)$ esu. Since the nonlinearity of the glass host is much weaker than that of the gold inclusions, the effective cubic susceptibility is given by the generalized (although truncated) Maxwell Garnett result

$$\chi^{(3)} = f q_i^2 |q_i|^2 \chi_i^{(3)}, \tag{9}$$

where the subscripts i and h denote inclusion and host values, respectively, while f represents the (metal) volume concentration or fill fraction, and q_i is the local field factor in the inclusions. Since the measurements were performed very near the surface plasmon resonance frequency ω_s we have the approximate condition that $\epsilon_i'(\omega_s) = -2\epsilon_h'$ and the local field factor is given by[3]

$$q_i = \frac{\epsilon + 2\epsilon_h}{\epsilon_i + 2\epsilon_h} \approx \frac{3\epsilon_h'}{i\epsilon_i''} \tag{10}$$

for hosts like glass without significant linear absorption. Because q_i is mainly imaginary, the slope of Eq. (9) becomes negative and the cubic susceptibility of gold is sign reversed from that of the composite.[3] Using the values $f \approx 10^{-5}$ and $\epsilon_h = 2.16$ we therefore obtain $\chi_i^{(3)} = (-1 \times 10^{-8} + 5 \times 10^{-8} i)$ esu. Hence, $\mathrm{Im}\,\chi^{(3)}/\mathrm{Re}\,\chi^{(3)} \approx -5$ and the solution is isolated to the lower half plane of Fig. 6, specifically to the fourth quadrant. This analysis therefore suggests a sign reversal in the real part upon transformation to susceptibilities but not in the imaginary part.

In summary, for gold we thus have $n_2'' > 0$ (by deduction and confirmed by the direct measurement herein) and $n_2' > 0$ (by deduction only, unconfirmed here due to low signal strength). Transforming to susceptibilities we have $\mathrm{Im}\,\chi^{(3)} > 0$ (no sign change) and $\mathrm{Re}\,\chi^{(3)} < 0$ (sign change), which isolates the possible values of the nonlinear coefficients to the part of the hyperbola extending into the fourth quadrant of Fig. 6. Note that the largest possible ratio of the refractive to absorptive nonlinearity in this quadrant is $n_2'/n_2'' = 5$. Then why is a satisfactory signal from the closed-aperture *z*-scan experiment not observed? There may be several reasons. For the same magnitude nonlinearity (that is, for $n_2' = n_2''$) deviations from the baseline ($T = 1$) are larger by a factor of approximately 3.5 for open-aperture scans than for closed-aperture scans. Moreover, the aperture transmittance tends to be small which further decreases the already small S/N ratio. Lastly, the effects of nonlinear absorption must be divided out of the resulting closed aperture scan, which for best results requires a third detector, and tends to further obscure any refractive nonlinearity.

CONCLUSIONS

The value of the nonlinear absorption coefficient was found through direct measurement on a gold film rather than on a composite structure. The obtained value is representative of bulk Au because the sample is continuous and because the film thickness is sufficient to avoid quantum size effects. Measurement of the constituent nonlinear susceptibilities is necessary for proper application and evaluation of effective medium theories for describing gold nanoparticle composites. However, we have shown that transformation of the experimentally determined nonlinear refractive indices to nonlinear susceptibilities is complicated by the coupling of real to imaginary quantities provided by the strong linear absorption of the metal. Hence, both open- and closed-aperture *z* scans must be performed to determine either the real or imaginary parts of the nonlinear susceptibility. However, closed-aperture *z* scans did not resolve a signal, and therefore we could not determine the nonlinear susceptibility properly. If we naively (and improperly) ignore the earlier-mentioned coupling, then the direct measurement made herein agrees well with the typical values obtained for the

nonlinear susceptibility of gold deduced from measurements on low concentration composites,[3,5,6] and also agrees well with the theoretically derived value for bulk gold based on thermalization of conduction electrons (which also ignores the coupling).[6] In the low concentration limit, effective medium theories tend to predict the behavior of the composite properly. However, at higher inclusion concentrations, effective medium theories significantly diverge from one another and likely do not produce the correct results (although they may provide general trends).

Notably the sign of the third-order susceptibility for the gold film was found to be reversed from that found previously for gold nanoparticle composites (below the percolation threshold). Previously, we demonstrated a counterintuitive consequence of local field effects that occurs in metal nanoparticle composites at the surface plasmon resonance.[3,6] Remarkably, although $\chi^{(3)}$ may be positive for each component by itself, $\chi^{(3)}$ may be negative for the composite as a whole. The finding herein is therefore a verification of this counterintuitive consequence of local fields, through a measurement of the nonlinearity of bulk Au by transmission. The physical origin of this sign reversal is presumably linked to the drastic change in conductivity that occurs at the percolation threshold.

Taken together, the results of the AFM, STM, conductivity, and transmittance measurements indicate that the 50 Å Au film is continuous. The extent of continuity determines whether a plasmon peak will be observed in the transmittance spectrum as well as whether the material will demonstrate saturable or induced absorption. Percolation structures tend to diminish the plasmon resonance and favor induced absorption. Hence, there is a strong correlation between thin film microstructure and optical properties, which in many cases is even more evident for nonlinear optical interactions which depend more strongly on geometrically determined local field factors.

ACKNOWLEDGMENTS

The authors gratefully acknowledge discussions with N. Halas, D. O. Henderson, R. Averitt, M. S. Paley, and D. O. Frazier on the contents of this work and the invaluable assistance of T. Kim, C. Banks, and W. Lu. This research was supported by the Center Director's Discretionary Fund and the Space Products Development Office at Marshall Space Flight Center, the Alliance for Microgravity Materials Science and Applications, the National Science Foundation, and the Army Research Office.

[1] D. Ricard, P. Rousignol, and C. Flytzanis, Opt. Lett. **10**, 511 (1985).
[2] H. B. Liao, R. F. Xiao, J. S. Fu, P. Yu, G. K. L. Wong, and P. Sheng, Appl. Phys. Lett. **70**, 1 (1997).
[3] D. D. Smith, G. Fischer, R. W. Boyd, and D. A. Gregory, J. Opt. Soc. Am. B **14**, 1625 (1997).
[4] K. Puech, W. Blau, A. Grund, C. Bubeck, and G. Cardenas, Opt. Lett. **20**, 1613 (1995).
[5] M. J. Bloemer, J. W. Haus, and P. R. Ashley, J. Opt. Soc. Am. B **7**, 790 (1990).
[6] F. Hache, D. Ricard, C. Flytzanis, and U. Kreibig, Appl. Phys. A: Solids Surf. **47**, 347 (1988).
[7] K. L. Chopra, *Thin Film Phenomena* (McGraw-Hill, New York, 1969), p. 163.
[8] P. A. DiMilla, J. P. Folkers, H. A. Biebuyek, and G. M. Whitesides, J. Am. Chem. Soc. **117**, 2225 (1994).
[9] C. V. Fragstein and H. Romer, Z. Phys. **151**, 54 (1958).
[10] T. Kim, R. M. Crooks, M. Tsen, and L. Sun, J. Am. Chem. Soc. **117**, 3963 (1995).
[11] C. A. Goss, D. H. Charych, and M. Majda, Anal. Chem. **63**, 85 (1991).
[12] M. Sheik-Bahae, A. A. Said, T. Wei, D. J. Hagan, and E. W. Van Stryland, IEEE J. Quantum Electron. **26**, 760 (1990).
[13] J. A. Giordmaine and J. A. Howe, Phys. Rev. Lett. **11**, 207 (1963).
[14] E. Palik, *Handbook of Optical Constants of Solids* (Academic Press, Orlando, FL, 1985), p. 286.
[15] M. L. Theye, Phys. Rev. B **2**, 3060 (1970).
[16] L. B. Valdes, Proc. IRE **42,** 420 (1954).
[17] P. Sheng, Phys. Rev. Lett. **45**, 60 (1980).